Secretory expression of mammalian NOTCH tandem epidermal growth factor-like repeats based on increased O-glycosylation

Ailing Zhang [a,b,c], Yohei Tsukamoto [a], Hideyuki Takeuchi [a,b,d], Kimitoshi Nishiwaki [c], Yuko Tashima [a,b], Tetsuya Okajima [a,b,*]

[a] *Department of Molecular Biochemistry, Nagoya University Graduate School of Medicine, Nagoya, Japan*
[b] *Institute for Glyco-core Research (iGCORE), Nagoya University, Nagoya, Japan*
[c] *Department of Anesthesiology, Nagoya University Graduate School of Medicine, Nagoya, Japan*
[d] *Department of Biochemistry, University of Shizuoka School of Pharmaceutical Sciences, Shizuoka, Japan*

ARTICLE INFO

ABSTRACT

The Notch pathway represents evolutionarily conserved intercellular signaling essential for cell–to–cell communication during development. Dysregulation of Notch signaling has been implicated in various diseases, and its control represents a potential cancer treatment strategy. Notch signaling is initiated by the interaction of NOTCH receptors with their ligands on neighboring cells. Therefore, the truncated NOTCH ectodomain, composed mainly of tandem repeats of epidermal growth factor-like (EGF) domains, serves as a decoy molecule that competes for ligand binding and thus inhibits ligand-dependent Notch signaling. Although full-length NOTCH EGF repeats exhibited potent Notch inhibitory activity, they were poorly produced in the transfected cells. This study evaluated the effect of EGF domain-modifying glycosyltransferases on the secretion of NOTCH EGF repeats. Our results in HEK293T cells revealed that, unlike the effect on endogenous NOTCH receptors, overexpressed EGF domain-specific O-GlcNAc transferase (EOGT) markedly enhanced the secretion of NOTCH1 EGF repeats in an enzyme activity-dependent manner. The co-expression of protein O-glucosyltransferase 1 further manifested the effect of EOGT. The resultant changes in O-glycosylation of NOTCH3 were evaluated by label-free glycopeptide quantification. This study provides an experimental strategy to efficiently generate NOTCH EGF repeats by manipulating the expression of glycosyltransferases that alter the O-glycosylation of EGF domains.

1. Introduction

Dysregulation of Notch signaling is associated with various cancers [1]. Although Notch signaling has both tumor-promoting and tumor-suppressive roles, it is considered a potential therapeutic target for tumors because tumor angiogenesis depends on Notch signaling; disruption of Notch signaling inhibits tumor growth by impairing angiogenesis [2]. Thus, establishing effective strategies to inhibit Notch signaling is of therapeutic importance. A previous study developed a soluble form of the NOTCH1 receptor (NOTCH1 decoy) that inhibits ligand-induced Notch signaling and tumor angiogenesis in vivo [3].

Although the NOTCH1 decoy molecule consists exclusively of a tandem array of epidermal growth factor-like (EGF) repeats, the expressed proteins are poorly secreted into the culture media and are predominantly retained within the cells. This is presumably because NOTCH1 consists of a large amount of EGF repeats (i.e., more than 30). The partial fragments of NOTCH1 EGF repeats, which are minimal binding units required for physical interaction with either Delta-like (DLL) or Jagged ligands, were more efficiently secreted into the culture medium [4]. This is a potential drawback in producing full-length NOTCH1 EGF repeats that can potentially act as pan-Notch inhibitors.

NOTCH EGF repeats are modified with specific O-glycans, including

O-fucose, O-glucose, and O-GlcNAc [5–8]. These glycosylations occur in the endoplasmic reticulum (ER) via specific glycosyltransferases, including protein O-fucosyltransferase 1 (POFUT1), protein O-gluco-syltransferase 1 (POGLUT1), and EGF domain-specific O-GlcNAc transferase (EOGT). Previous studies have revealed that POFUT1 and POGLUT1 affect the cell surface expression of endogenous NOTCH1 in various cell types, including HEK293T cells [9,10]. Furthermore, an expression vector encoding POFUT1 was used to promote secretion of NOTCH1 fragments in HEK293S cells [11]. Thus, optimal expression of EGF domain-specific glycosyltransferases may improve the production of full-length NOTCH EGF repeats. However, no comprehensive analysis has been conducted to date.

In this study, we evaluated the effects of overexpressed EGF domain-specific O-glycosyltransferases, including POFUT1, POGLUT1, and EOGT, on the secretion of NOTCH EGF repeats in HEK293T cells. Our results reveal a novel function of EOGT in promoting the secretion of recombinantly expressed NOTCH1 EGF repeats. Together with the development of a simplified methodology for comparative glyco-proteomics of O-glycans on NOTCH1 EGF repeats, this study provides a compelling approach to produce NOTCH EGF repeats based on the engineered expression of glycosyltransferases that increased their O-glycan modifications.

2. Material and methods

2.1. Antibodies and reagents

The antibodies used were as follows: anti-EOGT/AER61 (EPR12944) (1:10,000; Abcam #ab190693), anti-FLAG (1:1000; Wako #018–22386), anti-α-tubulin (12G10) (1:3000; DSHB), anti-c-Myc (9E10) (DSHB, 1:1000), HRP-conjugated anti-mouse IgG (Thermo-Fisher, 1:10,000), PE-conjugated anti-NOTCH1 (HMN1-12) (Biolegend #130608, 1:50), APC-conjugated anti-human Delta-like protein 4 (DLL4) antibody (MHD4-46) (Biolegend #346508, 1:100), HRP-conjugated anti-human IgG-Fc (Bethyl #A80-104P, 1:50,000), and HRP-conjugated anti-rabbit IgG (Cell signaling #7074P2, 1:10,000). The NOTCH3 expression vector (pCMV-Sport6-NOTCH3) was a gift from Michael Wang and obtained from Motoyuki Ito (Chiba University) [12]. The expression vectors encoding mouse POGLUT1 and mouse POFUT1 (pCMV6/POGLUT1:MycDDK and pCMV6/POFUT1:MycDDK) were obtained from Origene. The expression vectors for EOGT, EOGT^{R377Q}, and a control vector (pSectag2C/Eogt-IRES-GFP, pSectag2C/Eogt^{R377Q}-IR-ES-GFP, and pSectag2C/Eogt-IRES-GFP) have been described previously [13–15]. The expression vector for human IgG-Fc has been described previously [10,16].

2.2. Plasmid constructs

To construct the human DLL4 expression vector, cDNA prepared from HEK293 cells was subjected to PCR using the primer set described in Supplemental Fig. S1. The amplified products were digested with *Eco*RI and *Not*I and inserted into the pTracer-CMV vector. To generate an expression vector for FLAG:NOTCH1 EGF repeats, plasmids encoding mouse NOTCH1 were subjected to PCR, using the primers shown in Supplemental Fig. S1. The amplified product (nucleotide numbers 2735–4283: amino acid sequence 912–1428) digested with *Cla*I and *Xba*I was replaced with the fragment generated by the *Cla*I/*Xba*I digestion of pTracer-CMV-FLAG-Notch$^{119-1916}$ [17]. To create the L-FRINGE:Myc construct, plasmids encoding human L-FRINGE (pCMV-Entry6-L-FRINGE:Myc-FLAG) were subjected to PCR using the primers shown in Supplemental Fig. S1. The amplified product was digested with *Kpn*I and *Sac*II and replaced with the fragment generated by the *Kpn*I/*Sac*II digestion of pCMV-Entry6-L-Fringe:MycFLAG (Origene). To create an expression vector for human FLAG:NOTCH3 EGF repeats, human NOTCH3 from EGF domain 1 to LNR domain 1 (nucleotide numbers 118–4221: amino acid sequence 40–1407) was amplified

by PCR using primers described in Supplemental Fig. S1. Following digestion with *Afe*I/*Xba*I, the fragment was inserted into the pTracer-CMV vector [15]. The POGLUT1^{R279W} [18] mutant was generated by site-directed mutagenesis using the KOD-Plus Mutagenesis Kit (Toyobo). All the constructs were confirmed by DNA sequencing.

2.3. Cell culture and transfection

HEK293T cells were kindly provided by Matsuda T (Nagoya University, Japan). Cells were cultured in Dulbecco's Modified Eagle's Medium (DMEM) supplemented with 10% heat-inactivated fetal bovine serum (FBS) and 1% penicillin-streptomycin, at 37 °C and 5% CO_2. Expression vectors were transiently transfected using polyethyleneimine (PEI MAX, MW 40,000, Polysciences) and OPTI-MEM without FBS and antibiotics, as previously described [19]. One microgram of plasmid DNA was added to 100 μL OPTI-MEM and mixed with 5 μg of PEI in 100 μL of OPTI-MEM, followed by 20 min incubation at 23–25 °C. The DNA/PEI mixture was then added to the cells in 6 well plates washed with 1 ml of OPTI-MEM. After 6–18 h of incubation at 37 °C with 5% CO_2, the medium was supplemented with 1 ml of OPTI-MEM/DMEM mixtures containing 3% FBS and 0.3% penicillin-streptomycin. The cells were incubated for another 48–72 h before analysis.

2.4. Immunoblotting

Cells were lysed in a buffer containing 20 mM Tris-HCl, pH7.4, 150 mM NaCl, and 1% NP-40 with a protease inhibitor (cOmplete mini EDTA free, #11836170001, Roche). The lysates were denatured using SDS-PAGE sample buffer containing 2-mercaptoethanol, separated by 7.5% SDS-PAGE, and transferred onto a PVDF membrane (Millipore). The membrane was blocked in blocking buffer consisting of 5% skim milk in PBS/0.05% Tween 20 (PBS-T) at 23–25 °C for 30–60 min, followed by incubation with the appropriate primary antibody diluted in blocking buffer at 23–25 °C for 1 h or at 4 °C for 12 h. After washing three times with PBS-T for 10 min each, the membrane was incubated with horse-radish peroxidase (HRP)-conjugated secondary antibody in blocking buffer at 23–25 °C for 1 h. After the membrane was washed three times with PBS-T for 10 min each, the desired bands were visualized with Immobilon Western Chemiluminescent HRP Substrate (Millipore) and X-ray film (Fujifilm) or iBright1500 (Thermo Fisher Scientific). The intensity of each band was measured with ImageJ software.

2.5. Ligand binding assay

Culture media containing FLAG-tagged NOTCH1-EGF repeats was collected after 72 h incubation at 37 °C and 5% CO_2. After removing debris by centrifugation, the pH was adjusted to 7.4 with HEPES buffer. The culture medium was concentrated 1000 fold using an Amicon Ultra-15 centrifugal filter unit (50 kDa NMWCO; Millipore). The concentrated media was mixed with the same volume of ligand-binding buffer (Hanks' buffered salt solution, pH 7.4, 1 mM $CaCl_2$, 1% BSA, 0.05% NaN_3). DLL4-expressing HEK293T cells were stripped with PBS by pipetting at 4 °C and washed with a ligand-binding buffer. Cells were incubated with medium containing the NOTCH1-EGF repeats (100 μl) at 4 °C for 1 h. After washing with ligand binding buffer, cells were cultured with PE-conjugated Notch1 (1:50 in ligand binding buffer) and APC-conjugated DLL4 (1:100 in ligand binding buffer) at 4 °C for 25 min. Cells were washed with 1 ml of ligand-binding buffer and analyzed using a BD FACSCanto II flow cytometer (BD Biosciences).

2.6. Hybrid quadrupole FT linear ion trap MS analysis

Recombinant FLAG-tagged NOTCH3 EGF repeats were transiently expressed in HEK293T cells using PEI MAX as described above. The next day, the cells were washed with fresh culture medium and cultured for three days. The collected medium was incubated with DDDDK-tagged

Protein PURIFICATION GEL (#3328R, MBL). After washing with a solution containing 50 mM Tris-HCl, pH7.4, 150 mM NaCl, and 0.1% NP-40, the proteins bound onto the agarose beads were eluted using SDS sample buffer (133 mM Tris-HCl, pH6.8, 2.2% SDS, 11.1% glycerol, and 0.01% bromophenol blue). The samples were reduced by adding tris(2-carboxyethyl)phosphine (TCEP) at a final concentration of 7.2 mM and heated at 100 °C for 5 min. For alkylation, samples were incubated with iodoacetamide dissolved in 50 mM Tris-HCl, pH6.8, for 1 h at 23–25 °C. The samples were subjected to SDS-PAGE and stained with GelCode Blue Stain Reagent (Thermo Fisher Scientific). The stained bands containing the NOTCH fragment were excised and transferred to low-binding protein tubes (InaOptica). The gels were washed with 50% methanol-20 mM diammonium phosphate (DiAP) for 1 h at 23–25 °C with rotation, and the supernatant was removed. The remaining gel was washed with 50% methanol-20 mM DiAP and rotated at 4 °C overnight. The washing was repeated three times with 50% methanol-20 mM DiAP for 1 h with rotation at 23–25 °C. Acetonitrile was added to the gel, incubated for 30 min, and dried. Samples were incubated with 0.03 mg/ml trypsin (Promega) diluted in 20 mM DiAP for 5 h at 37 °C. Digested peptides were extracted with acetonitrile containing 0.1% formic acid and desalted using a Ziptip (Millipore).

The peptides were analyzed using an Orbitrap Fusion Tribrid mass spectrometer (Thermo Fisher Scientific) coupled to an UltiMate 3000 RSLC nano-LC system (Dionex Co.) equipped with a nano-HPLC capillary column via a nanoelectrospray ion source, as described previously [20]. Data-dependent tandem MS analysis was performed using a top-speed approach (cycle time, 3 s). The precursor ions were analyzed using an Orbitrap mass analyzer, whereas the fragment ions generated by HCD fragmentation were analyzed using a linear ion trap mass analyzer. The data acquisition parameters are summarized in Supplemental Fig. S2.

2.7. Qualitative and semi-quantitative analysis of O-GlcNAc and O-Glc Glycans

Peak lists were generated using extract_msn in Xcalibur 3.0.6 (Thermo Scientific) with the default parameters. Data analysis was performed using Proteome Discoverer (version 2.3) and Byonic node (version 1.0.376). The following input files and parameters were specified: human NOTCH3 (Uniprot ID: Q9UM47 [Last modified February 23, 2022]) amino acid sequence [40–1373] as a peptide sequence, trypsin (specific for cleavage at the C-terminus of Lys/Arg) as a proteolytic enzyme with the possibility of two missed cleavages, carbamidomethylation of Cys residues as a fixed modification, and methionine oxidation and β–hydroxylation of Asn/Asp as variable modifications. MS/MS search and scoring was performed using the following parameters: MS1 tolerance, 20 ppm; MS/MS tolerance, 0.5 Da; HCD mode. Data processing workflow in Proteome Discoverer software is shown in Supplemental Fig. S3. The parameter settings of the precursor ion quantifier node of Proteome Discoverer and the Byonic node are reported in Supplemental Fig. S4. Peak height was selected for quantification.

The extracted ion chromatograms (EICs) were generated using the Xcalibur Qual browser, as described previously [20]. The EIC peak height was measured and compensated for by the isotope abundance ratio. The relative intensities derived from all the observed charge states of each glycopeptide were summed. The proportion of integrated peak height values for the specified glycoforms to those corresponding to all detectable (glyco-)peptides was calculated for semi-quantification. The glycoproteome data in this study were deposited in jPOST (Project ID: JPST001694).

3. Results and discussion

3.1. Exogenously expressed EOGT promotes the secretion of EGF repeats of NOTCH1

Based on a previous study showing that EOGT promotes the DLL4-NOTCH1 interaction [19], we exogenously expressed EOGT to prepare a culture medium containing NOTCH1 EGF repeats. We focused on HEK293T cells because it is a standard cell line generally used for protein expression and production. The plasmid construct encoding the entire NOTCH1 EGF repeat with an N-terminal FLAG tag (FLAG:N1-EGF) was generated and transfected into HEK293T cells with or without EOGT. Culture media containing FLAG:N1-EGF were incubated with DLL4 ligand-expressing cells. FACS analysis revealed that the amount of FLAG:N1-EGF bound to ligand-expressing cells markedly increased with EOGT overexpression (Fig. 1A). The effect on DLL4-binding is similar to that of L-FRINGE, which adds GlcNAc to O-fucose [21]. However, the amount of FLAG:N1-EGF in the culture media was elevated when co-expressed with EOGT, but not L-FRINGE (Fig. 1B). The effect of EOGT on NOTCH1 EGF repeats contrasts with its impact on endogenous NOTCH1, because NOTCH1 expression on the cell surface is unaffected by the lack of EOGT in HEK293T cells [19]. However, this is in line with the observation that EOGT could affect the cell surface expression of NOTCH1 in the sensitized condition where O-fucose or O-glucose modifications were removed from multiple EGF domains [17]. These results suggest that EOGT possesses a novel but seemingly physiologically irrelevant ability to promote the secretion of EGF repeats of NOTCH1, which at least partially contributes to increased binding to DLL4.

3.2. Enhanced secretion of NOTCH1 EGF repeats by co-expression of EOGT and POGLUT1

To analyze the amount of FLAG:N1-EGF secreted from the transfected cells, culture media and cell lysates were prepared and subjected to immunoblotting with an anti-FLAG antibody. Quantification was performed by calculating the amount of secreted FLAG:N1-EGF relative to that in cell lysates, which compensated for the transfection efficiency. Consistent with the above results, FLAG:N1-EGF secreted in the culture media was increased by co-expression of EOGT (2.37-fold increase; $p = 0.0509$), but not by L-FRING (Fig. 2A). The effect of EOGT was further supported by observations in *EOGT*-deficient cells, where co-expression of EOGT resulted in a profound increase in the secretion of FLAG:N1-EGF (4.18-fold increase; $p = 0.0092$) (Fig. 2B).

To explore the specificity of Notch-modifying glycosyltransferases in promoting FLAG:N1-EGF NOTCH1 secretion, we examined the combined effects of glycosyltransferases acting on EGF domains in the endoplasmic reticulum (ER), including POFUT1, POGLUT1, and EOGT. Previous studies have indicated that the *Drosophila* POFUT1 homolog (OFUT1) is essential for NOTCH expression on the cell surface [22]. In HEK293T cells, both POFUT1 and POGLUT1 play significant roles in cell surface expression of NOTCH1 [10]. Despite the roles of POFUT1 and POGLUT1 in the secretory pathway, the effect of POFUT1 or POGLUT1 overexpression on FLAG:N1-EGF NOTCH1 secretion was not statistically significant in HEK293T cells. In contrast, co-expression of EOGT/POGLUT1, but not EOGT/POFUT1, further increased secretion compared with EOGT alone (Fig. 2A). Similar results were obtained when *EOGT*-deficient cells were used (Fig. 2B). These results indicated that unlike the effect on endogenously expressed NOTCH1, overexpression of POGLUT1 exerted minor effects on the secretion of NOTCH1 EGF repeats, and POFUT1 exhibited negligible effects in HEK293T cells. Therefore, the optimal combination of ER-resident glycosyltransferases serves as a strategy for efficiently producing NOTCH1 EGF repeats in cultured cells.
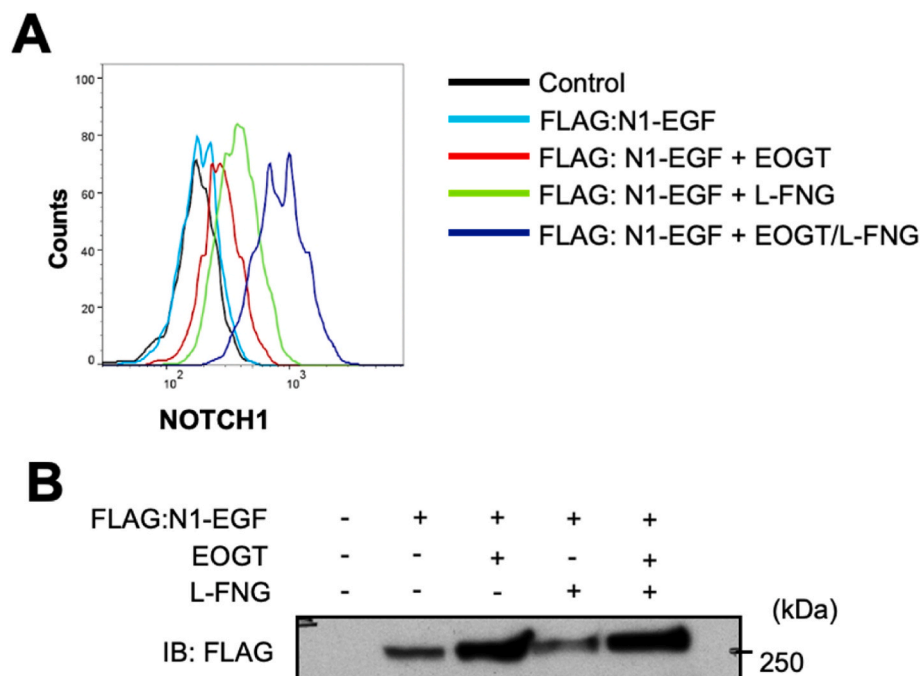
Fig. 1. DLL4-binding of NOTCH1 EGF repeats that were produced in cells transfected to express EOGT or L-FRINGE **(A)** FLAG:NOTCH1-EGF (FLAG:N1-EGF) was expressed in HEK293T cells with or without EOGT and L-FRINGE (L-FNG). Culture media was collected and incubated with HEK293T cells expressing DLL4. The amount of bound FLAG:N1-EGF in DLL4 positive cells was analyzed by flow cytometry with PE-conjugated NOTCH1 antibody. **(B)** Immunoblotting of culture media obtained from HEK293T cells expressing FLAG:N1-EGF with (+) or without (−) EOGT and L-FNG. Indicated antibodies were used for immunoblotting (IB).
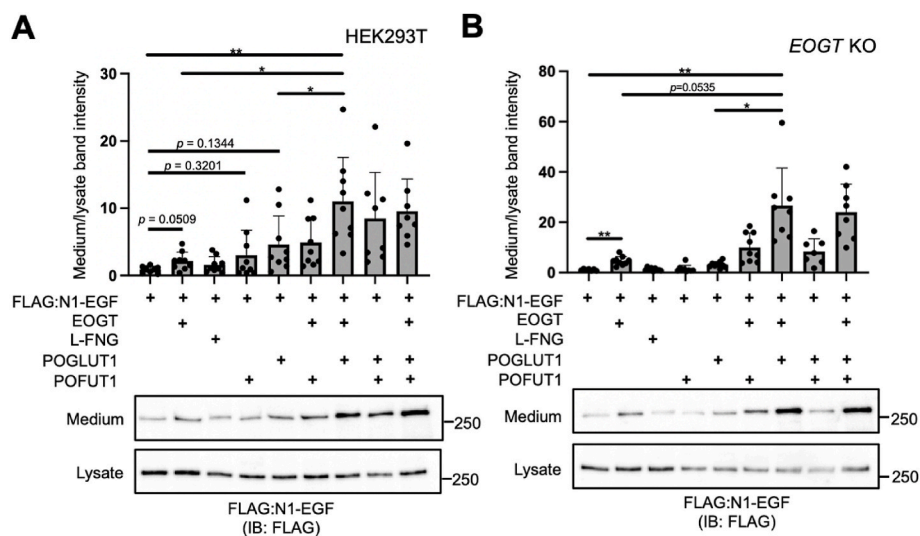

Fig. 2. FLAG:N1-EGF secretion in HEK293T cells was enhanced by co-transfection of EOGT and POGLUT1 **(A)** FLAG:N1-EGF was expressed in HEK293T cells in the presence or absence of indicated glycosyltransferases. For quantification, secreted FLAG:N1-EGF in culture media relative to that in cell lysates was measured by immunoblotting with FLAG antibodies. The data were expressed as mean ± standard deviation (SD) of the indicated number of samples (n = 8–9). *$p < 0.05$; **$p < 0.01$ (Tukey's multiple comparisons test). Representative immunoblots are shown below. **(B)** Same with (A) but in *EOGT*-deficient HEK293T cells.

3.3. Enzymatic activity of EOGT and POGLUT1 contribute to increased production of NOTCH1 EGF repeats

A previous study on *Drosophila* OFUT1 indicated that glycosyltransferases can promote NOTCH secretion in an enzyme activity-independent manner [22]. To address whether the effects of EOGT and POGLUT1 are mediated by their enzymatic activities, we analyzed the impact of enzymatically inactive mutants of these glycosyltransferases [14]. Quantification of secreted FLAG:N1-EGF from *EOGT* mutant HEK293T cells co-expressing inactive EOGT harboring the R377Q mutation showed that EOGT[R377Q] failed to facilitate secretion into the culture media (Fig. 3A and B). These data suggested that enzyme activity is essential for the effect of EOGT on the promotion of FLAG:N1-EGF secretion.

To address the requirement of O-glucosyltransferase activity of POGLUT1, we generated a POGLUT1[R279W] mutant associated with Dowling-Degos disease, which has been shown to be inactive in vitro

[23]. Co-expression of POGLUT1[R279W] slightly increased the secretion of FLAG:N1-EGF, but to a lesser extent than that of wild-type POGLUT1 (Fig. 3C and D). These data suggest that the increased O-glucosylation of NOTCH1 partly contributes to the secretion of NOTCH1 EGF repeats.

3.4. Co-expression of EOGT and POGLUT1 facilitates the secretion of NOTCH3 EGF repeats

To explore whether co-expression of EOGT and POGLUT1 improves the secretion of other NOTCH receptors besides NOTCH1, a FLAG epitope tag was fused to the N-terminal end of NOTCH3 tandem EGF repeats (FLAG:N3-EGF). Despite substantial differences in the amount of secreted proteins, FLAG:N3-EGF secretion was significantly increased by co-expression of EOGT and POGLUT1 (Fig. 4A and B). The specific effect on NOTCH EGF repeats was confirmed by monitoring the secretion of human IgG-Fc (Fig. 4C and D). These results support the effectiveness of this strategy for the efficient production of EGF repeats of various
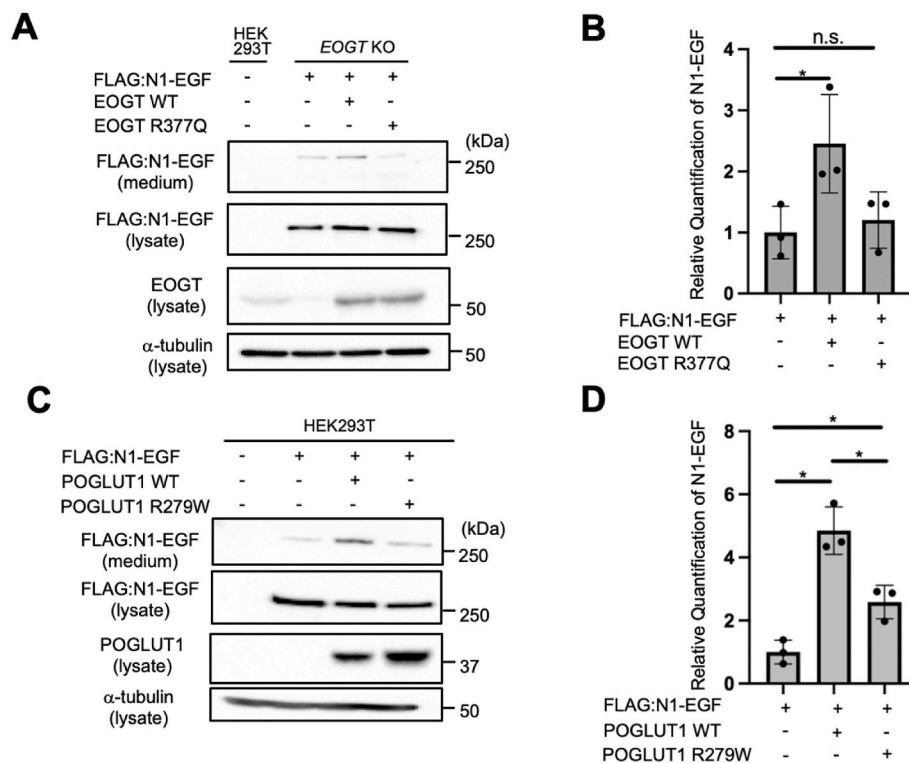
Fig. 3. Enzymic activities for EOGT and POGLUT1 mediate enhanced FLAG:N1-EGF secretion **(A)** FLAG: N1-EGF was co-transfected with wild-type EOGT or the R377Q mutant. Immunoblotting (IB) was performed with indicated antibodies. **(B)** FLAG:N1-EGF secretion in the culture media relative to cell lysates was measured by immunoblotting with a FLAG antibody. The data were expressed as mean ± standard deviation (SD) of triplicate samples. *$p < 0.05$ (Dunnett's multiple comparisons test). **(C)** FLAG:N1-EGF were co-expressed with POGLUT1 or the R279W mutant. Immunoblotting was performed with indicated antibodies. **(D)** Same with (B) but with wild-type POGLUT1 or the R279W mutant. *$p < 0.05$ (Tukey's multiple comparisons test).
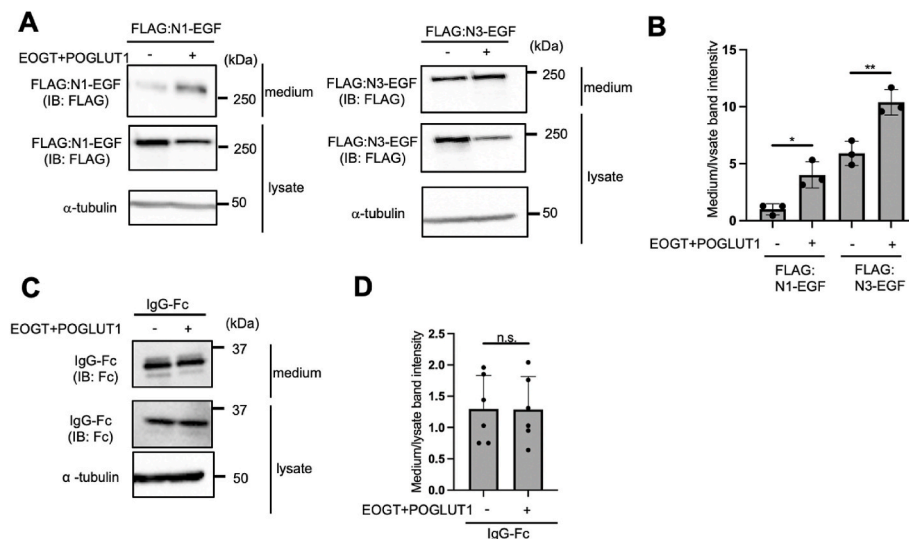

Fig. 4. EOGT and POGLUT1 promote secretion of NOTCH3 EGF repeats construct **(A)** FLAG:N1-EGF or FLAG:N3-EGF was co-transfected with EOGT and POGLUT1 in HEK293T cells. Immunoblotting (IB) was performed with indicated antibodies. **(B)** Secreted NOTCH EGF repeats construct in culture media relative to that in cell lysates was analyzed by immunoblotting with a FLAG antibody. The data were expressed as mean ± standard deviation (SD) of triplicate samples. *$p < 0.05$; **$p < 0.01$ (Student's t-test). **(C–D)** Same as (A–B) but for IgG-Fc.

NOTCH family members based on the engineered expression of glycosyltransferases.

3.5. Co-expression of EOGT and POGLUT1 increased the O-glycosylation of FLAG:N3-EGF

To evaluate changes in the O-glycosylation states of EGF repeats mediated by the co-expression of EOGT and POGLUT1, mass spectrometric analysis was performed. We selected FLAG:N3-EGF for analysis because of the abundance of the purified proteins (Fig. 4B). There are no comprehensive studies on O-glycans on NOTCH3 [24] whereas glycoproteomic analysis of NOTCH1 has been extensively investigated [16, 20,25]. In these studies, O-glycans on NOTCH1 were semi-quantitatively analyzed based on extracted ion chromatograms (EICs), which require

manual processing of the obtained mass spectrometry datasets.

To simplify the methodology for the comparative analysis of glycopeptides from FLAG:N3-EGF, we adopted the label-free quantitation workflow in Proteome Discoverer with Byonic node, a search engine suitable for glycopeptide identification from MS/MS spectra [26,27]. A list of the identified glycosylated and unglycosylated peptides is provided in Supplemental Table S1. It should be noted that this workflow cannot evaluate glycopeptides containing multiple O-glycosylation sites, which were manually removed from the summary tables (Fig. 5A). The results from Proteome Discoverer, which quantifies multiple isotopic clusters, were parallel with our EIC-based methods that quantify the most abundant isotopic peaks and are normalized for the isotope abundance ratio (Fig. 5B and C) [16,20,25].

Consistent with the O-GlcNAc transferase activity of EOGT, the

A Peptides containing O-GlcNAc modification sites

EGF domain	Position in Protein	Annotated Sequence	Glycan Composition	Other modifications	Abundance Ratio	Abundances Cont.	Abundances EOGT+POGLUT1	Theo. MH+ [Da]	m/z [Da]	Top Apex RT [min]
EGF4	183	[R].CQCPAGYTGPLCENPAVPCAPSPCR.[N]	HexNAc(1)	5xCarbamidomethyl; 1xOxidation	0.5	2614399	1326681	3038.257	1013.424	27.76
EGF4	183	[R].CQCPAGYTGPLCENPAVPCAPSPCR.[N]	HexNAc(1)Hex(1)	5xCarbamidomethyl	1.2	2049875	2414860	3184.315	1062.110	27.82
EGF4	183	[R].CQCPAGYTGPLCENPAVPCAPSPCR.[N]	HexNAc(1)	5xCarbamidomethyl	1.2	20149286	23192351	3022.262	1008.093	27.96
EGF4	183	[R].CQCPAGYTGPLCENPAVPCAPSPCR.[N]		5xCarbamidomethyl	0.0	831307		2819.183	940.399	28.42
EGF9	375	[R].AICTCPPGFTGGACDQDVDECSIGANPCEHLGR.[C]	HexNAc(1)Hex(1)	5xCarbamidomethyl	6.8	1832462	12375055	3986.624	997.413	28.15
EGF9	375	[R].AICTCPPGFTGGACDQDVDECSIGANPCEHLGR.[C]	HexNAc(1)	5xCarbamidomethyl	7.4	2647541	19463024	3824.571	956.899	28.25
EGF9	375	[R].AICTCPPGFTGGACDQDVDECSIGANPCEHLGR.[C]	HexNAc(1)	5xCarbamidomethyl; 1xOxidation	0.1	2091376	289640	3637.487	910.127	28.38
EGF9	375	[R].AICTCPPGFTGGACDQDVDECSIGANPCEHLGR.[C]	HexNAc(1)Hex(1)NeuAc(1)	5xCarbamidomethyl	12.4	1397868	17355809	4277.720	856.350	28.51
EGF9	375	[R].AICTCPPGFTGGACDQDVDECSIGANPCEHLGR.[C]		5xCarbamidomethyl	0.4	32817366	13086865	3621.492	906.129	28.52
EGF10	422	[R].GYTGPR.[C]	HexNAc(1)Hex(1)		100.0		175621	1015.458	508.232	21.8
EGF10	422	[R].GYTGPR.[C]	HexNAc(1)		27.7	13037	360923	853.405	427.206	21.93
EGF14	559	[R].CVDGIASFSCACAPGYTGTR.[C]	HexNAc(1)Hex(1)	3xCarbamidomethyl; 1xOxidation	0.4	2810057	1166731	2531.037	844.351	28.65
EGF14	559	[R].CVDGIASFSCACAPGYTGTR.[C]	HexNAc(1)	3xCarbamidomethyl; 1xOxidation	2.1	10839653	23194830	2368.984	1184.997	28.77
EGF14	559	[R].CVDGIASFSCACAPGYTGTR.[C]		3xCarbamidomethyl; 1xOxidation	0.8	497363	398388	2165.905	1083.456	28.77
EGF14	559	[R].CVDGIASFSCACAPGYTGTR.[C]		3xCarbamidomethyl	0.0	88785		2149.910	717.309	29.05
EGF18	718	[R].CVCEPGWSGPR.[C]	HexNAc(1)Hex(1)	2xCarbamidomethyl	1.1	3390551	3737550	1669.683	835.346	25.98
EGF18	718	[R].CVCEPGWSGPR.[C]	Hex(1)	2xCarbamidomethyl	100.0	63947		1466.604	733.806	26.08
EGF18	718	[R].CVCEPGWSGPR.[C]	HexNAc(1)	2xCarbamidomethyl	1.4	6810496	9255612	1507.630	754.319	26.11
EGF18	718	[R].CVCEPGWSGPR.[C]		2xCarbamidomethyl	0.5	2121962	1017881	1304.551	652.780	26.45
EGF18	718	[R].CVCEPGWSGPR.[C]	HexNAc(1)Hex(1)NeuAc(1)	2xCarbamidomethyl	0.6	144448	80288	1960.779	980.892	26.7
EGF25	986	[R].CTCLESFTGPQCCQTLVDWCSR.[Q]	HexNAc(1)	4xCarbamidomethyl; 1xOxidation	100.0		1044685	2824.168	942.062	30.08
EGF25	986	[R].CTCLESFTGPQCCQTLVDWCSR.[Q]	HexNAc(1)	4xCarbamidomethyl	6.1	2775733	16968631	2808.173	936.730	30.43
EGF25	986	[R].CTCLESFTGPQCCQTLVDWCSR.[Q]		4xCarbamidomethyl; 1xOxidation	0.3	772912	2621.089	874.368	30.68
EGF25	986	[R].CTCLESFTGPQCCQTLVDWCSR.[Q]		4xCarbamidomethyl	0.1	17954220	958177	2605.094	869.036	31
EGF26	1015	[R].CVQTGAYCLCPPGWSGR.[L]	Hex(1)	3xCarbamidomethyl	100.0		983628	2130.904	1065.955	29.07
EGF26	1015	[R].CVQTGAYCLCPPGWSGR.[L]		3xCarbamidomethyl	0.6	13241974	8098932	1968.851	984.929	29.39
EGF30	1191	[R].CTCPPGYTGLR.[C]	HexNAc(1)	2xCarbamidomethyl	1.5	5795494	8897592	1484.651	742.830	25.55
EGF30	1191	[R].CTCPPGYTGLR.[C]		2xCarbamidomethyl	0.8	2193024	1736442	1281.571	641.290	25.55
EGF31	1232	[R].CLCHAGFSGPR.[C]	HexNAc(1)Hex(1)	2xCarbamidomethyl	18.9	93205	1759703	1626.689	542.901	24.33
EGF31	1232	[R].CLCHAGFSGPR.[C]	HexNAc(1)	2xCarbamidomethyl	11.1	155679	1729603	1464.636	488.883	24.4
EGF31	1232	[R].CLCHAGFSGPR.[C]		2xCarbamidomethyl	1.0	6407737	6175629	1261.556	421.190	24.59
EGF33	1313	[R].CACPPGLSGPSCR.[S]		3xCarbamidomethyl	1.9	5456946	10551005	1418.597	709.803	25.16
EGF34	1361	[R].CACAQGWTGPR.[C]	HexNAc(1)	2xCarbamidomethyl	100.0		302564	1466.615	733.812	24.94
EGF34	1361	[R].CACAQGWTGPR.[C]		2xCarbamidomethyl	1.2	6516889	8085518	1263.536	632.272	25.34

Peptides containing O-Glc modification sites

| EGF domain	Position in Protein	Annotated Sequence	Glycan Composition	Other modifications	Abundance Ratio	Abundances Cont.	Abundances EOGT+POGLUT1	Theo. MH+ [Da]	m/z [Da]	Top Apex RT [min]
EGF2	76	[R].CQLEDPCHSGPCAGR.[G]	Hex(1)	3xCarbamidomethyl; 1xOxidation	1.4	232398	330497	1921.747	641.255	23.28
EGF2	76	[R].CQLEDPCHSGPCAGR.[G]	Hex(2)	3xCarbamidomethyl	100.0		12527	2067.805	689.939	23.54
EGF2	76	[R].CQLEDPCHSGPCAGR.[G]	Hex(1)	3xCarbamidomethyl	1.3	3221601	4276744	1905.752	635.923	23.67
EGF2	76	[R].CQLEDPCHSGPCAGR.[G]	Hex(1)Pent(1)	3xCarbamidomethyl	1.0	39170	37423	2037.795	679.937	23.71
EGF2	76	[R].CQLEDPCHSGPCAGR.[G]	Hex(1)Pent(2)	3xCarbamidomethyl	1.3	32761	43861	2169.837	723.951	23.73
EGF2	76	[R].CQLEDPCHSGPCAGR.[G]		3xCarbamidomethyl	1.1	49857	54689	1743.700	581.905	24
EGF11	428	[R].CETDVNECLSGPCR.[N]	Hex(1)Pent(2)	3xCarbamidomethyl; 1xOxidation	0.8	496210	406026	2138.805	1069.906	24.69
EGF11	428	[R].CETDVNECLSGPCR.[N]	Hex(1)	3xCarbamidomethyl	27.6	52890	1425583	1858.725	929.867	25.04
EGF11	428	[R].CETDVNECLSGPCR.[N]	Hex(1)Pent(1)	3xCarbamidomethyl	1.8	340765	613636	1990.767	995.888	25.05
EGF11	428	[R].CETDVNECLSGPCR.[N]	Hex(1)Pent(2)	3xCarbamidomethyl	1.0	9493620	9861200	2122.810	708.276	25.05
EGF11	428	[R].CETDVNECLSGPCR.[N]		3xCarbamidomethyl	0.9	380777	351799	1696.672	848.840	25.44
EGF15	588	[R].SGPSCR.[H]	Hex(1)Pent(2)	1xCarbamidomethyl	1.2	50754	61280	1073.430	537.219	20.23
EGF19	736	[R].DACESQPCR.[A]	Hex(1)	2xCarbamidomethyl	1.2	405706	504421	1284.483	642.746	20.66
EGF19	736	[R].DACESQPCR.[A]	Hex(1)Pent(1)	2xCarbamidomethyl	2.0	12553	25025	1416.525	708.767	20.81
EGF19	736	[R].DACESQPCR.[A]	Hex(1)Pent(2)	2xCarbamidomethyl	1.1	23344	25362	1548.568	774.788	20.91
EGF32	1243	[R].CQTVLSPCESQPCQHGGQCR.[P]	Hex(1)	4xCarbamidomethyl	1.0	1578063	1527594	2551.043	851.019	24.33
EGF32	1243	[R].CQTVLSPCESQPCQHGGQCR.[P]	Hex(1)Pent(1)	4xCarbamidomethyl	1.7	47078	79244	2683.085	895.367	24.42
EGF32	1243	[R].CQTVLSPCESQPCQHGGQCR.[P]		4xCarbamidomethyl	0.4	286314	112866	2388.990	797.002	24.56
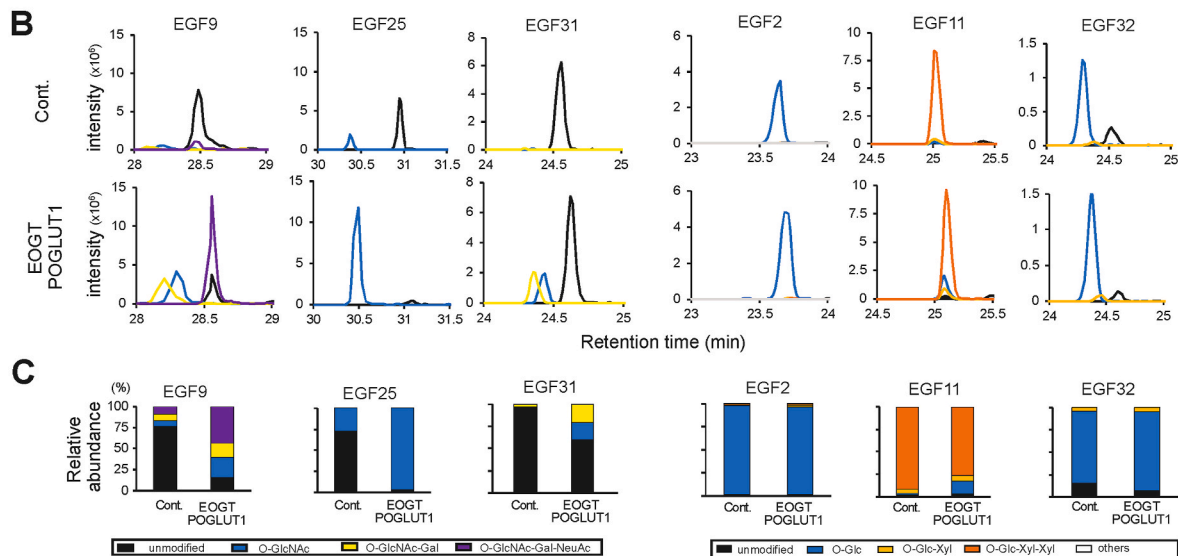
Fig. 5. Altered O-glycosylation states of NOTCH3 EGF repeats by overexpressing EOGT and POGLUT1. HEK293T cells were transfected with FLAG:N3-EGF, with or without EOGT/POGLUT1. The tryptic digests of FLAG:N3-EGF were analyzed using LC-MS/MS. **(A)** Proteome Discoverer and Byonic node were used to perform comparative glycoproteomics of O-GlcNAc and O-Glc glycans. It is noted that peptides containing multiple O-glycosylation sites were manually removed from the list because of the uncertainty of their respective modifications. Abundance ratio was calculated by dividing the abundance value of the EOGT + POGLUT1 sample (Abundances EOGT + POGLUT1) by the value of the control sample (Abundances Cont.). Data of one representative experiment are shown. Similar results were obtained in two independent experiments (Supplemental Table S1). **(B)** Extracted ion chromatograms (EICs) of glycopeptides containing O-Glc and O-GlcNAc sites. The left graphs (EGF9, 25, and 31) represent the data corresponding to unmodified peptides (*black*) or glycopeptides modified with O-GlcNAc (*blue*), O-GlcNAc-Gal (*yellow*), or O-GlcNAc-Gal-NeuAc (*purple*). The right graphs (EGF2, 11, and 32) represent data corresponding to unmodified peptides (black) or glycopeptides modified with O-Glc (*blue*), O-Glc-Xyl (*light orange*), or O-Glc-Xyl-Xyl (*orange*) glycans. **(C)** Semi-quantitative measurement of glycopeptides modified with O-GlcNAc or O-Glc glycans based on the EICs shown in (B). (For interpretation of the references to colour in this figure legend, the reader is referred to the Web version of this article.)

abundance ratio of HexNAc-modified glycopeptides corresponding to O-GlcNAc, O-GlcNAc-Gal, or O-GlcNAc-Gal-NeuAc glycoforms was markedly increased at EGF9, 10, 25, 31, and 34 by EOGT/POGLUT1 overexpression (Fig. 5A). These data support our proposal that elevated O-GlcNAc modifications promote the secretion of NOTCH EGF repeats.

In contrast, the effect on EGF4, 14, 18, and 30 was limited because O-GlcNAcylation occurs at high stoichiometries regardless of the exogenously expressed glycosyltransferases. These constitutive O-GlcNAc modifications on NOTCH3 possibly contribute to the secretion of its EGF repeats in wild-type HEK293T cells as with NOTCH1 EGF repeats (Fig. 2).

Unlike in the case of O-GlcNAc modification, the effect of EOGT/POGLUT1 on O-Glc modification was obscure, because all detectable O-Glc sites on FLAG:N3-EGF were mostly O-glycosylated without EOGT/POGLUT1 overexpression (Fig. 5A). Similarly, a previous study showed that most O-Glc sites on NOTCH1 expressed in wild-type HEK293T cells were modified with O-Hex at high stoichiometries [16]. These results were somewhat contradictory to the enzyme activity-dependent effect of POGLUT1 on FLAG:N1-EGF secretion (Fig. 3D). It should be noted, however, that NOTCH EGF repeats with insufficient O-glycosylation are not secreted and therefore not detected by mass spectrometry of secreted proteins in culture medium. Expression of POGLUT1 may reduce the proportion of insufficiently O-glucosylated NOTCH EGF, which is otherwise retained in the cells. The molecular mechanisms underlying the actions of POGLUT1 require further investigation.

The analytical method presented in this study can be applied to other glycoproteins to analyze the effect of engineered expression of glycosyltransferases that lead to altered O-glycosylation. The evaluation of O-glycosylation states is particularly critical for NOTCH receptors, whose stability and ligand-binding ability are modulated by O-glycans on their EGF repeats.

4. Conclusion

The Notch signaling pathway is precisely controlled during animal development, and dysregulation of this pathway is associated with various diseases, including cancer. NOTCH EGF repeats serve as decoy molecules that are expected to interact with ligands and thus inhibit ligand-dependent Notch signaling, which is expected to disrupt tumor angiogenesis. Although full-length NOTCH EGF repeats exhibit potent Notch inhibitor activity, they are poorly secreted from cells compared to partial EGF repeats in cultured cells. This study suggests that combining ER-resident EGF domain-specific glycosyltransferases improved the amount of secreted NOTCH EGF repeats in the culture media. Notably, we showed for the first time that EOGT has the potential to promote the secretory expression of NOTCH EGF repeats. We speculated that overexpressing these glycosyltransferases is effective in the sensitized condition where NOTCH EGF repeats are prone to be under-O-glycosylated. The altered O-glycosylation states of NOTCH EGF repeats were evaluated by mass spectrometry using the simplified label-free quantitation workflow of Proteome Discoverer. These strategies are applicable to the production and quality control of full-length NOTCH EGF repeats for use as pharmaceuticals effective against diseases, including various cancers [28].

CRediT authorship contribution statement

AZ: Visualization, investigation, data curation, formal analysis, resources, methodology, validation, writing - original draft preparation. YoT: Visualization, investigation, data curation, formal analysis, resources, methodology, and validation. HT: Funding acquisition, project administration, supervision, validation, writing, review, and editing. KN: Project administration and supervision. YuT: Visualization, investigation, data curation, formal analysis, resources, methodology, and validation. TO: conceptualization, funding acquisition, project administration, supervision, writing - original draft preparation, writing -

review, and editing.

Declaration of competing interest

The authors declare that there is no conflict of interest.

Data availability

Data will be made available on request.

Appendix A. Supplementary data

Supplementary data related to this article can be found at https://doi.org/10.1016/j.ab.2022.114881.

References

[1] O. Meurette, P. Mehlen, Notch signaling in the tumor microenvironment, Cancer Cell 34 (4) (2018) 536–548.

[2] J. Dufraine, Y. Funahashi, J. Kitajewski, Notch signaling regulates tumor angiogenesis by diverse mechanisms, Oncogene 27 (38) (2008) 5132–5137.

[3] Y. Funahashi, S.L. Hernandez, I. Das, A. Ahn, J. Huang, M. Vorontchikhina, et al., A notch1 ectodomain construct inhibits endothelial notch signaling, tumor growth, and angiogenesis, Cancer Res. 68 (12) (2008) 4727–4735, https://doi.org/10.1158/0008-5472.CAN-07-6499. Epub 2008/06/19, PubMed PMID: 18559519; PubMed Central PMCID: PMCPMC3690602.

[4] T. Kangsamaksin, A. Murtomaki, N.M. Kofler, H. Cuervo, R.A. Chaudhri, I. W. Tattersall, et al., NOTCH decoys that selectively block DLL/NOTCH or JAG/NOTCH disrupt angiogenesis by unique mechanisms to inhibit tumor growth, Cancer Discov. 5 (2) (2015) 182–197, https://doi.org/10.1158/2159-8290.Cd-14-0650. PubMed PMID: WOS:000349393600026.

[5] P. Stanley, T. Okajima, Roles of glycosylation in Notch signaling, Curr. Top. Dev. Biol. 92 (2010) 131–164, https://doi.org/10.1016/S0070-2153(10)92004-8. Epub 2010/09/08, PubMed PMID: 20816394.

[6] H. Takeuchi, R.S. Haltiwanger, Significance of glycosylation in Notch signaling, Biochem. Biophys. Res. Commun. 453 (2) (2014) 235–242.

[7] M. Ogawa, T. Okajima, Structure and function of extracellular O-GlcNAc, Curr. Opin. Struct. Biol. 56 (2019) 72–77, https://doi.org/10.1016/j.sbi.2018.12.002. Epub 2019/01/23, PubMed PMID: 30669087.

[8] P.-W. Lo, T. Okajima, Eogt-catalyzed O-GlcNAcylation, Trends Glycosci. Glycotechnol. 34 (197) (2022) E1–E6.

[9] R. Ajima, E. Suzuki, Y. Saga, Pofut1 point-mutations that disrupt O-fucosyltransferase activity destabilize the protein and abolish Notch1 signaling during mouse somitogenesis, PLoS One 12 (11) (2017), e0187248.

[10] H. Takeuchi, H.J. Yu, H.L. Hao, M. Takeuchi, A. Ito, H.L. Li, et al., O-Glycosylation modulates the stability of epidermal growth factor-like repeats and thereby regulates Notch trafficking, J. Biol. Chem. 292 (38) (2017) 15964–15973, https://doi.org/10.1074/jbc.M117.800102. PubMed PMID: WOS:000411512200032.

[11] M.B. Andrawes, X. Xu, H. Liu, S.B. Ficarro, J.A. Marto, J.C. Aster, et al., Intrinsic selectivity of notch 1 for delta-like 4 over delta-like 1, J. Biol. Chem. 288 (35) (2013) 25477–25489.

[12] H. Meng, X. Zhang, G. Yu, S.J. Lee, Y.E. Chen, I. Prudovsky, et al., Biochemical characterization and cellular effects of CADASIL mutants of NOTCH3, PLoS One 7 (9) (2012), e44964, https://doi.org/10.1371/journal.pone.0044964. Epub 2012/10/03, PubMed PMID: 23028706; PubMed Central PMCID: PMCPMC3445613.

[13] Y. Sakaidani, N. Ichiyanagi, C. Saito, T. Nomura, M. Ito, Y. Nishio, et al., O-linked-N-acetylglucosamine modification of mammalian Notch receptors by an atypical O-GlcNAc transferase Eogt1, Biochem. Biophys. Res. Commun. 419 (1) (2012) 14–19, https://doi.org/10.1016/j.bbrc.2012.01.098. Epub 2012/02/09, PubMed PMID: 22310717.

[14] M. Ogawa, S. Sawaguchi, T. Kawai, D. Nadano, T. Matsuda, H. Yagi, et al., Impaired O-linked N-acetylglucosaminylation in the endoplasmic reticulum by mutated epidermal growth factor (EGF) domain-specific O-linked N-acetylglucosamine transferase found in Adams-Oliver syndrome, J. Biol. Chem. 290 (4) (2015) 2137–2149, https://doi.org/10.1074/jbc.M114.598821. PubMed PMID: 25488668; PubMed Central PMCID: PMC4303666.

[15] S.M.D. Alam, Y. Tsukamoto, M. Ogawa, Y. Senoo, K. Ikeda, Y. Tashima, et al., N-Glycans on EGF domain-specific O-GlcNAc transferase (EOGT) facilitate EOGT maturation and peripheral endoplasmic reticulum localization, J. Biol. Chem. 295 (25) (2020) 8560–8574, https://doi.org/10.1074/jbc.RA119.012280. Epub 2020/05/08, PubMed PMID: 32376684; PubMed Central PMCID: PMCPMC7307186.

[16] Y. Urata, W. Saiki, Y. Tsukamoto, H. Sago, H. Hibi, T. Okajima, et al., Xylosyl extension of O-glucose glycans on the extracellular domain of NOTCH1 and NOTCH2 regulates notch cell surface trafficking, Cells 9 (5) (2020), https://doi.org/10.3390/cells9051220. Epub 2020/05/20, PubMed PMID: 32423029; PubMed Central PMCID: PMCPMC7291291.

[17] M. Ogawa, Y. Tashima, Y. Sakaguchi, H. Takeuchi, T. Okajima, Contribution of extracellular O-GlcNAc to the stability of folded epidermal growth factor-like domains and Notch1 trafficking, Biochem. Biophys. Res. Commun. 526 (1) (2020) 184–190, https://doi.org/10.1016/j.bbrc.2020.03.066. Epub 2020/03/24, PubMed PMID: 32201074.

[18] D.J. Ralser, H. Takeuchi, G. Fritz, F.B. Basmanav, M. Effern, S. Sivalingam, et al., Altered notch signaling in dowling-degos disease: additional mutations in POGLUT1 and further insights into disease pathogenesis, J. Invest. Dermatol. 139 (4) (2019) 960–964, https://doi.org/10.1016/j.jid.2018.10.030. Epub 2018/11/12, PubMed PMID: 30414910; PubMed Central PMCID: PMCPMC6431572.

[19] S. Sawaguchi, S. Varshney, M. Ogawa, Y. Sakaidani, H. Yagi, K. Takeshita, et al., O-GlcNAc on NOTCH1 EGF repeats regulates ligand-induced Notch signaling and vascular development in mammals, Elife 6 (2017). PubMed PMID: Medline: 28395734.

[20] Y. Tsukamoto, M. Ogawa, K. Yogi, Y. Tashima, H. Takeuchi, T. Okajima, Glycoproteomics of NOTCH1 EGF repeat fragments overexpressed with different glycosyltransferases in HEK293T cells reveals insights into O-GlcNAcylation of NOTCH1, Glycobiology 32 (7) (2022) 616–628.

[21] S. Yu, W. Wang, M. Albakri, X. Yu, G. Majihail, S. Lim, et al., O-Fucose and Fringe-modified NOTCH1 extracellular domain fragments as decoys to release niche-lodged hematopoietic progenitor cells, Glycobiology 31 (5) (2021) 582–592.

[22] T. Okajima, A. Xu, L. Lei, K.D. Irvine, Chaperone activity of protein O-fucosyltransferase 1 promotes notch receptor folding, Science 307 (5715) (2005) 1599–1603.

[23] D.J. Ralser, H. Takeuchi, G. Fritz, F.B. Basmanav, S. Sivalingam, et al., Altered Notch signaling in Dowling-Degos disease: additional mutations in POGLUT1 and further insights into disease pathogenesis, J. Invest. Dermatol. 139 (4) (2019) 960.

[24] J.F. Arboleda-Velasquez, R. Rampal, E. Fung, D.C. Darland, M. Liu, M.C. Martinez, et al., CADASIL mutations impair Notch3 glycosylation by Fringe, Hum. Mol. Genet. 14 (12) (2005) 1631–1639.

[25] S. Kakuda, R.S. Haltiwanger, Deciphering the fringe-mediated notch code: identification of activating and inhibiting sites allowing discrimination between ligands, Dev. Cell 40 (2) (2017) 193–201, https://doi.org/10.1016/j.devcel.2016.12.013. Epub 2017/01/17, PubMed PMID: 28089369; PubMed Central PMCID: PMCPMC5263050.

[26] M. Bern, Y.J. Kil, C. Becker, Byonic: advanced peptide and protein identification software, Current protocols in bioinformatics 40 (1) (2012), 13.20. 1-13.20. 14.

[27] H. Hashiguchi, Y. Tsukamoto, M. Ogawa, Y. Tashima, H. Takeuchi, M. Nakamura, et al., Glycoproteomic analysis identifies cryptdin-related sequence 1 as O-glycosylated protein modified with α1, 2-fucose in the small intestine, Arch. Biochem. Biophys. 695 (2020), 108653.

[28] W. Wang, T. Okajima, H. Takeuchi, Significant roles of notch O-glycosylation in cancer, Molecules 27 (6) (2022) 1783.